wjert, 2024, Vol. 10 Issue 5, 107-119. Review Article ISSN 2454-695X

World Journal of Engineering Research and Technology
WJERT
www.wjert.org

SJIF Impact Factor: 7.029

SYNCHRONIZATION BEHAVIOR OF LAMINAR CHAOS BASED ON A STAR-COUPLED MODEL

Quo Qiang Qiu*

School of Science, Jiangxi University of Science and Technology, Ganzhou, Jiangxi, China.

Article Received on 04/03/2024 **Article Revised on 24/03/2024** **Article Accepted on 14/04/2024**

***Corresponding Author**
Quo Qiang Qiu
School of Science, Jiangxi University of Science and Technology, Ganzhou, Jiangxi, China.

ABSTRACT

Laminar chaos, as an emerging type of chaos, is different from traditional chaos. It has a chaotically varying laminar phase and is periodically interrupted by irregular bursts. By modulating laminar chaos through a star-coupled system, we find that when the time-varying time-lag amplitude of the system is mismatched, the oscillators exhibit oscillatory synchronization behaviors (laminar region is completely synchronized, and the sequence values of the chaotic region are alternately transformed) as the coupling strength reaches a certain threshold, but the difference between the peripheral oscillators is smaller than that between the central oscillator and the peripheral oscillators. These findings deepen our understanding of the laminar flow chaotic synchronization and regulation mechanisms, and open up new perspectives for the study of the synchronization behavior of chaotic systems. Future studies can explore the synchronization characteristics under different parameter conditions and apply these findings to practical engineering and technological fields, thus promoting the development of related fields.

KEYWORDS: Laminar chaos; laminar chaos synchronization; oscillation synchronization; star coupling.

1. INTRODUCTION

Time delay is a pervasive phenomenon in nature and in several scientific fields, including control theory,[1,2] chaos control,[3,4] engineering,[5,6] chemistry,[7] biology,[8] and life sciences.[9] Such delays are primarily due to limitations in the rate of information transfer and

reaction time of dynamic systems. The existence of time delays leads to a range of complex and fascinating phenomena, such as bifurcation,[10] chaotic behavior[11] and multistability of systems,[12] which provide a window to deeply understand and explore the dynamic behavior of systems.

We know relatively little about the dynamics of time-varying time-delay systems compared to systems with constant time lag. Recent studies have rigorously explored time-varying time-lag systems and clarified the concepts of conservative and dissipative delays.[13] In this context, David et al.[14] moderated the periodic dynamics of length and the chaotic dynamics of intensity level by introducing two one-dimensional mappings in a scalar system and found that the periodic dynamics and the chaotic dynamics of intensity level in a scalar system demonstrated that the outputs of systems with time-varying delays can exhibit a novel chaotic behavior, discovering a new chaotic state and naming it as called laminar chaos. Laminar chaos, as defined in Refs.[14] is an oscillation with a laminar phase characterized by irregular periodic interruptions of the amplitude which are chaotically distributed. This is significantly different from conventional chaos.

With the discovery of laminar chaos, it attracted a large number of scholars to flock into it and study it in various aspects, for example, in 2019 Joseph D as well as David et al. observed laminar chaos for the first time in optoelectronic experiments with time-varying delays at the same time proved its robustness,[15] Thomas et al. investigated the dissipative delays and conserved delays in the experiments of a double-diode nonlinear circuit and found that in this system is capable of laminar mixing; in the same year,[16] DD et al. from the Russian Academy of Sciences conducted the first experimental study of laminar chaos in a radio-engineering delay-feedback generator, in which the delay time is modulated by an external harmonic signal.[17] The regions of existence of various laminar flow chaotic states in the plane of external excitation parameters were mapped. The nonlinear function of the generator in the laminar flow chaotic state is reconstructed. Its existence in natural systems is further confirmed.

However, at present, most of the domestic and international studies on laminar chaos are on how to observe or test the laminar chaos itself under the influence of time lag, and few studies have been conducted on the synchronization behavior of this new type of chaos. Vladimir et al. in 2021 explored the behavior of laminar chaos in self-oscillating ring systems and focused on analyzing its stability under different delay modes, which provided important

insights for understanding the complex behavior of chaotic systems. important insights, and also concluded that two laminar chaotic systems are capable of generating oscillatory synchronization behavior (complete synchronization of laminar regions and alternating sequence value transformations in chaotic regions) under certain conditions[18]; In 2022 Taniya Khatun et al. made the first study of the synchronization behavior of laminar chaos, and found that the two systems are capable of going from generalized hysteresis to generalized expected synchronization to complete synchronization under different time delays. phenomenon and found essentially no similarity with the traditional chaotic synchronization phenomenon.[19] However, the synchronization behavior of laminar chaotic systems under other coupling modes has not been mentioned by scholars, so this study intends to conduct an in-depth study of laminar chaos through the star coupling mode, and to explore the synchronization behavior of laminar chaotic systems and their synchronization effects under the star coupling mode.

We consider a time-varying time-lag system and couple four such systems by means of a star-coupling model[20, 21] and find that, under the star-coupling approach, the system exhibits different synchronization effects with different parameter variations, and the results show that, for the system with inconsistent access mapping parameters, the oscillators exhibit oscillatory synchronization behaviors as the coupling strength reaches a certain threshold, but the difference between the peripheral oscillators is smaller than the difference between the center and peripheral oscillators.

2. Model of laminar chaos

Introducing a time-varying time-lag equation as in Eq. (1).

$$\alpha \cdot \dot{x}(t) + x(t) = f\left(x(R(t))\right) \#(1)$$

Where $R(t) = t - \tau(t)$ is the access mapping, which can also be called the delay parameter, and is one of the necessary conditions for generating into laminar flow chaos, and $\tau(t) = \tau_0 + \frac{A}{2\pi}\sin(2\pi t)$ is the time-varying delay with period 1.

The nonlinear function $f(x)$ is a generalized Logistic mapping, which is named Cubic mapping in this paper, in the following form

$$f(x) = \rho \cdot x(1 - x^2) \#(2)$$

where t is the iteration time step and ρ is a tunable parameter, since ρ determines the chaotic effect of the system, so in this paper, we refer to it as the chaotic observation value, by drawing the bifurcation diagram of this mapping, and at the same time numerically calculating its Lyapunov exponent, we can derive its chaotic region as shown in Fig. 1, when the Lyapunov exponent is greater than 0, i.e., when the chaotic observation value corresponding to the red region in the diagram can make the system produce chaos, and the interval of its chaotic observations is $\rho \in [2.52,3]$.

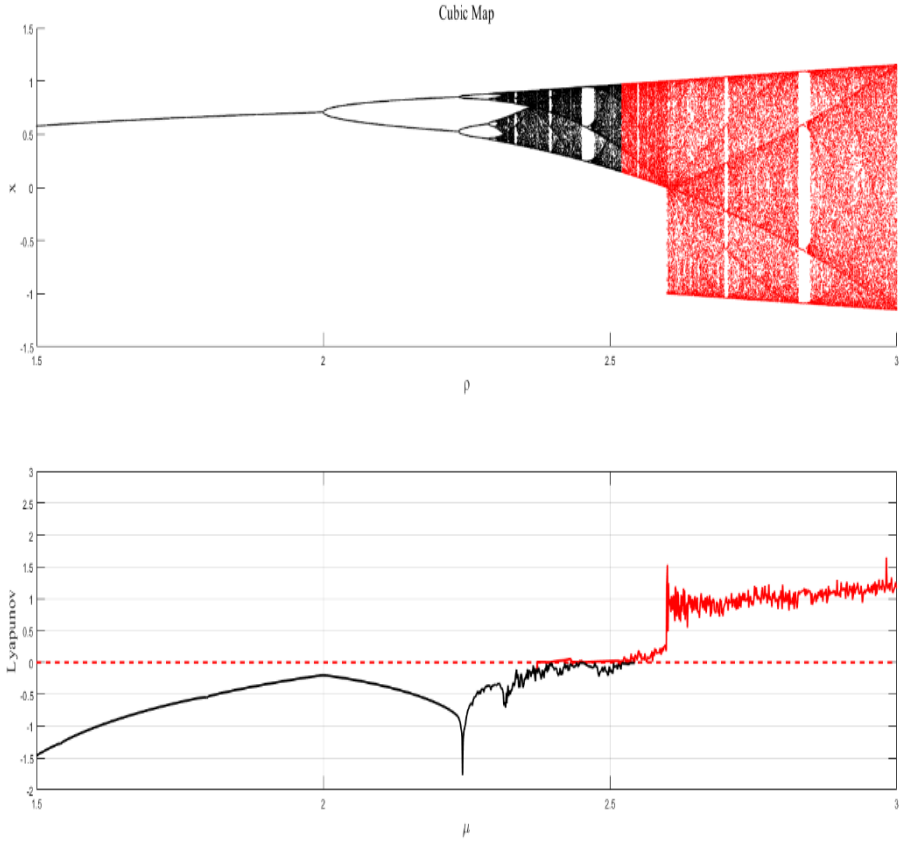

Fig. 1: Bifurcation plots of nonlinear functions, Lyapunov exponents, where red regions indicate that their Lyapunov exponents are greater than 0.

We validate Eq. (1) by numerical simulation through the fourth-order Lungkuta method with a step size of 0.0001, and we find that the chosen mapping is able to produce laminar chaos as shown in Fig. (2). When $\tau_0 = 1.5$, the system is dissipative delayed, which exhibits a laminar chaotic state as shown in Fig. 2(a), and when $\tau_0 = 1.54$, the system is conservative delayed, which exhibits a turbulent chaotic state as shown in Fig. 2(b) shown.

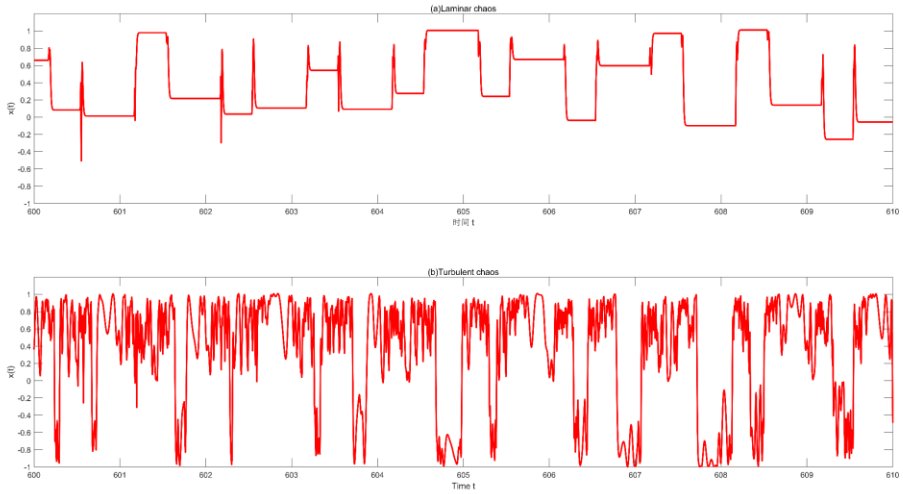

Fig. 2: Time series chart, where $A = 0.9, \rho = 2.63, \alpha = 0.05$ **(a),(b) the time delay** τ_0 **is1.50,1.54 respectively.**

3. Model of Star Coupling

The star coupling model is a mathematical model that describes the interaction of a multi-node system in which there is a coupling relationship between a central node and multiple peripheral nodes. To describe the star coupling model specifically, we can use a general coupling equation. Equation (3) is a simple formula for the star coupling model:

$$x_i = f(x_i) + \sum_{j=1}^{N} K_{ij} g(x_j - x_i) + \varepsilon \xi_i(t) \#(3)$$

Where: x_i denotes the state variable of the ith node, $f(x_i)$ is the internal dynamics equation of the node that describes the law of independent evolution of that node. n is the number of nodes, K_{ij} is the coupling strength between node i and node j, $g(x_j - x_i)$ describes the coupling function between the nodes, ε is the strength of the introduction of the external noise, and $\xi_i(t)$ is the agitated sound term.

Since this paper focuses on the linear coupling of N equal to 4, i.e., four laminar chaotic oscillators, the model of this star-shaped coupling can be represented by Fig. 3.

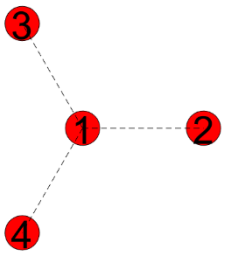

Fig. 3: Four-oscillator star coupling model.

In this paper, only this model is simulated, so let the noise term be constant equal to 0. Bringing the laminar flow chaotic system selected in this paper into Eq. (4), the following coupling equation is obtained.

$$\begin{cases} \alpha \dot{x_1}(t) = -x_1(t) + f_1\left(x_1(R_1(t))\right) + w[x_2(t) + x_3(t) + x_4(t) - 3x_1(t)] \\ \alpha \dot{x_2}(t) = -x_2(t) + f_2\left(x_2(R_2(t))\right) + w[x_1(t) - x_2(t)] \\ \alpha \dot{x_3}(t) = -x_3(t) + f_2\left(x_3(R_3(t))\right) + w[x_1(t) - x_3(t)] \\ \alpha \dot{x_4}(t) = -x_4(t) + f_4\left(x_4(R_4(t))\right) + w[x_1(t) - x_4(t)] \\ \# \end{cases} \quad \#(4)$$

Where $\alpha = 0.05$, characterizing the inertial properties of the system, is determined by the nonlinear function $f(x) = \rho x(1 - x^2)$, $R_1(t) = t - \tau_1(t)$, $R_2(t) = t - \tau_2(t)$,ω is the coupling coefficient, and ρ is the chaotic observation.

4. Study of system synchronization effects under inconsistent access mapping parameters

We study the synchronization effect and synchronization behavior of the coupled system under the star coupling model based on setting different amplitudes of the delay parameter in the access mapping parameter, respectively, setting the amplitude settings in the access mapping as $A1 = 0.9, A2 = 0.91, A3 = 0.92, A4 = 0.93$ and bringing into Eq. (4) to be verified in simulation by the fourth-order Lungerkuta method with the step size of 0.0001,. The following results are obtained.

As demonstrated by each oscillator sequence in Fig. 4(a), when the coupling strength is 0.5, the difference between the values of each oscillator sequence is large, which indicates that the system is in an unsynchronized state, but with the increase of the coupling strength, the values of the sequences are basically completely overlapped when the coupling strength is 1.2, but in the chaotic region, their values are not completely overlapped, and there is an error, as demonstrated in Fig. 4(b).

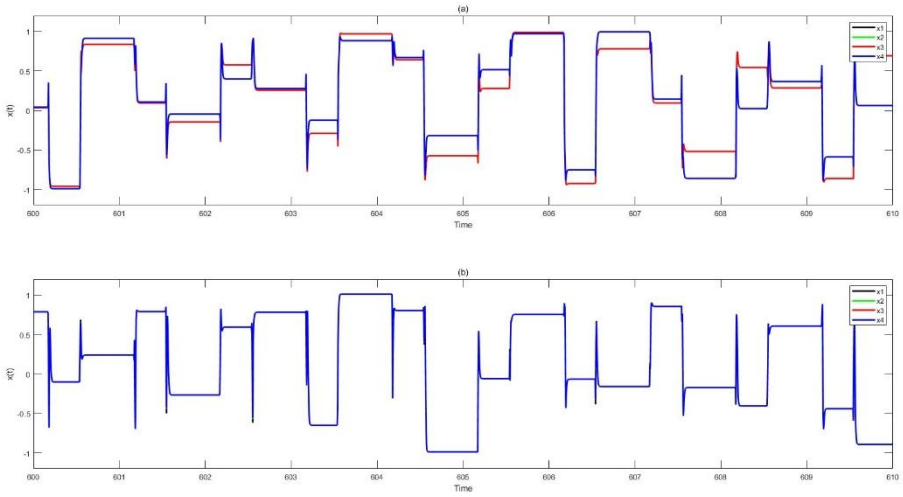

Fig. 4: (a),(b) Sequence diagrams of the oscillator corresponding to the coupling strengths $\omega = 0.5$, $\omega = 1.2$, respectively; where the black line is the sequence $x_1(t)$, the green line is $x_2(t)$, the red line is $x_3(t)$, and the blue line is $x_4(t)$, and the parameters are set as follows:$A1 = 0.9, A2 = 0.91, A3 = 0.92, A4 = 0.93$, $f(x) = \rho x(1 - x^2)$, $\rho = 2.63$.

In order to explore this reason, we further calculate the phase diagrams between the oscillators when the coupling strength is 1.2, and obtain the results shown in Fig. 5, where we find that the phase diagrams of its center oscillator, $x_1(t)$, and its peripheral oscillators, $x_2(t)$, $x_3(t)$, and $x_4(t)$, show a straight line variation around the slope of 1, which can be seen in Fig. 5(a,b,c); whereas the phase diagrams between the peripheral oscillators are direct straight line with slope 1, but there is still a small error, which can be seen in Fig. 5(d,e,f) It is thus concluded that in this coupled modulation system, the oscillators do not exhibit a fully synchronized behavior.

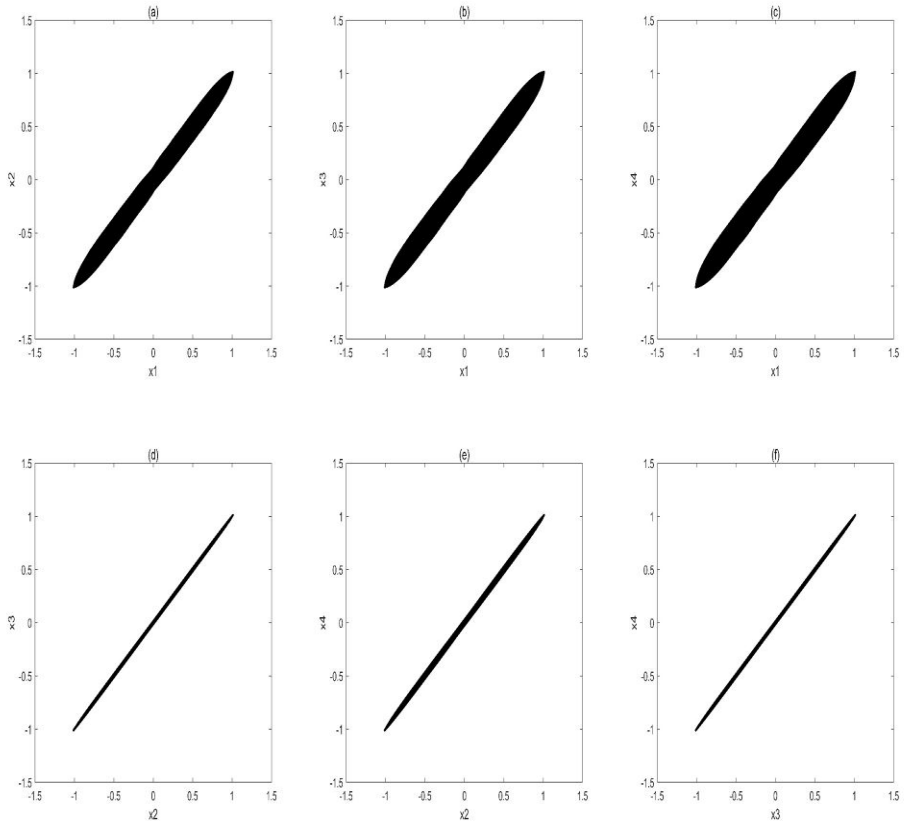

Fig. 5: Phase diagrams between each oscillator, where (a): oscillator $x_1(t)$, $x_2(t)$ phase diagram, (b): oscillator $x_1(t)$, $x_3(t)$ phase diagram, (c): oscillator $x_1(t)$, $x_4(t)$ phase diagram, (d): oscillator $x_2(t)$, $x_3(t)$ phase diagram, (e): oscillator $x_2(t)$, $x_4(t)$ phase diagram, and (f): oscillator$x_3(t)$, $x_4(t)$ phase diagram, when the coupling strength ω = 1.2.

However, we can observe in Fig. 4(b) that the oscillator sequences are partially synchronized in some regions, and in order to study it more deeply, we show the sequence difference of each oscillator in Fig. 6, Fig. 7 when the coupling strength is 1.2, and observing Fig. 6 we find that when the coupling strength is sufficiently large, the inter-oscillator difference is gradually hovering around 0. However, the difference between the center oscillator and the peripheral oscillators is significantly larger than that between the peripheral oscillators, and we also conclude that it does not show a completely synchronized state, but when we zoom in its sequence difference, we find that at coupling strength 1.2, the sequence difference of the system is completely 0 in the laminar region, and the difference in the chaotic region hovers around 0, forming the characteristic of oscillatory synchronization, please refer to Fig. 7(b).

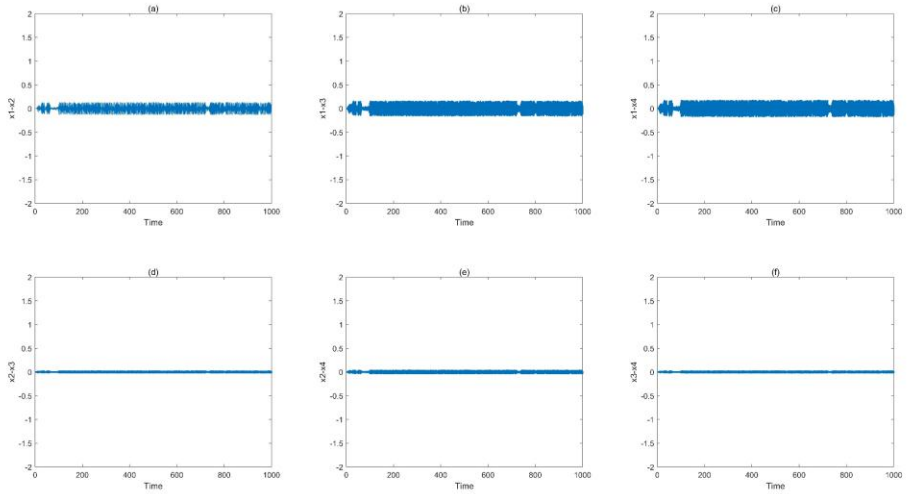

Fig. 6: Plot of the difference between each oscillator with respect to time, the horizontal coordinate is the time t, the vertical coordinate is the difference, where(a): $x_1(t) - x_2(t)$, **(b):** $x_1(t) - x_3(t)$, **(c):** $x_1(t) - x_4(t)$, **(d):** $x_2(t) - x_3(t)$, **(e):** $x_2(t) - x_4(t)$, **(a):** $x_3(t) - x_4(t)$, $\omega = 1.2$.

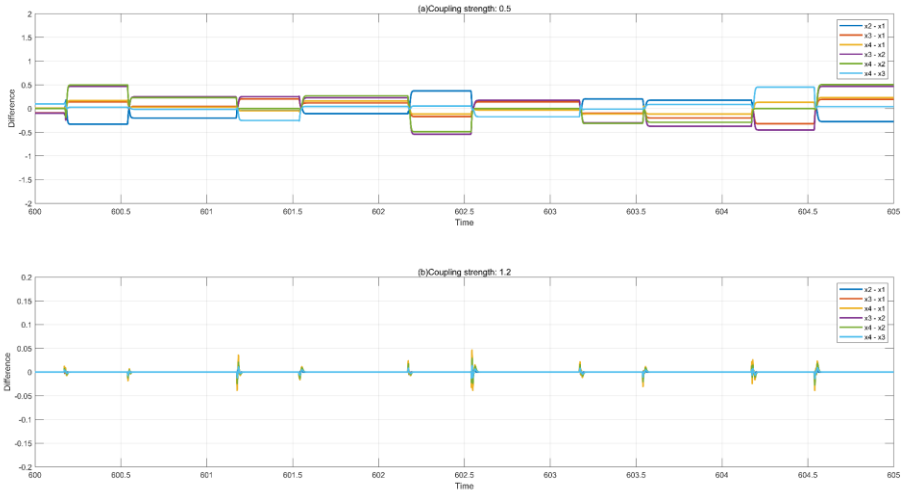

Fig. 7: Localized zoomed-in plots of sequence differences at different coupling strengths corresponding to (a): $\omega = 0.5$, **(b):** $\omega = 1.2$, **where (c) is a localized zoomed-in plot of Fig. 6.**

In order to comprehensively investigate the influence of the coupling strength on the synchronization behavior of the system, we continue to calculate the average difference of the difference of each sequence of differences in the system, as shown in Fig. 8, where the horizontal coordinate is the time t, the green, yellow, and brown lines denote the difference

between the peripheral oscillators, and the dark blue, blue, and violet lines denote the difference between the central oscillator and the peripheral triple oscillator), and it is found that with the gradual coupling strength enhancement, the difference between each oscillator constantly fluctuates and the fluctuation is not regular, but its difference gradually decreases, from the beginning of the fluctuation around 0.5 to 2 gradually decreases and stabilizes below 0.5, after the coupling strength is greater than 1.1, the difference of each oscillator sequence is stabilized at a certain plateau, but the difference between different oscillators stabilizes at the plateau of inconsistency, specifically, we find that the difference between the sequences $x_1(t)$ and $x_2(t), x_3(t), x_4(t)$ is significantly larger than that between $x_2(t), x_3(t), x_4(t)$, and the system is gradually stabilized after the coupling strength reaches a certain threshold, which leads to the conclusion that the coupling effect between peripheral oscillators is significantly higher than that between the center oscillator and peripheral oscillators in this coupling model. This difference does not change with the increase of the coupling strength.

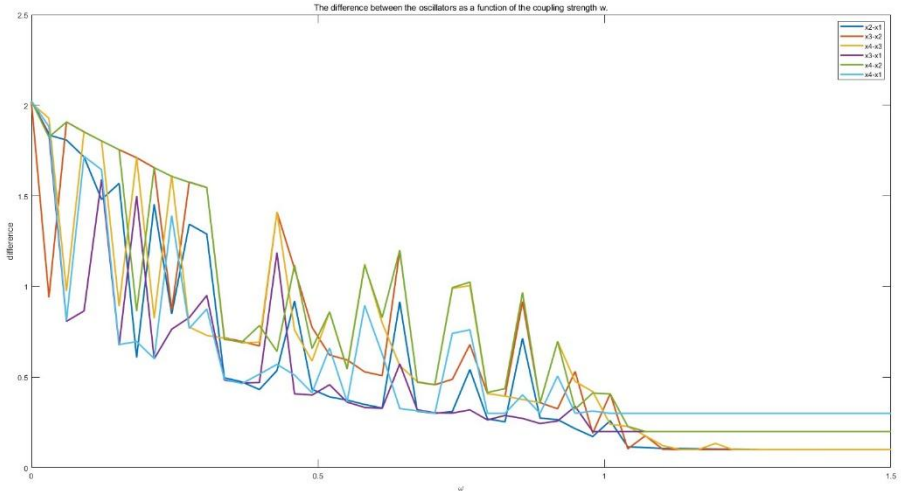

Fig. 8: The process of the variation of the mean difference between the vibrators of the system with the coupling strength is plotted as shown in the legend of Fig. Each line represents the mean difference between the vibrators respectively, and the form of the variation of the difference with the coupling strength remains basically the same. where $A1 = 0.9, A2 = 0.91, A3 = 0.92, A4 = 0.93$, $f(x) = \rho x(1 - x^2)$, $\rho = 2.63$.

In summary, it is concluded that under the laminar chaos in the star coupling model, with the increase of the coupling strength, the system gradually changes from unsynchronized to synchronized tendency, and the difference value between the oscillators fluctuates irregularly for a period of time, but after the coupling strength increases to 1.1, the coupling system is

gradually stabilized and the difference value of each oscillator is in the plateau stage, and the system finally exhibits the oscillatory synchronization, and at the same time, it is proved that the center of the oscillator and peripheral oscillators under star coupling are repulsive anisotropy originated from themselves, which is independent of the star coupling. It also confirms that the repulsive anisotropy between the center and peripheral vibrators under the star coupling originates from itself and has nothing to do with the coupling strength.

5. CONCLUSION

This paper reveals the diversity and complexity of the synchronization behaviors of the system under different coupling strength conditions through an in-depth study of the effects of the star-shaped coupling mode adopted by the four vibrators on the laminar flow chaotic model. An exhaustive discussion of the synchronization behavior of the laminar flow chaotic system under the four-vibrator star coupling model aims to deepen the understanding of the dynamical properties of the system under this special coupling structure. By systematically analyzing the synchronization behavior of the laminar chaotic system under different access mapping parameters, we find that the system transitions from an initial asynchronous state to an oscillatory synchronized state as the coupling strength increases, exhibiting intuitive evidence of the effect of the coupling strength on the synchronization process.

The experimental results further reveal that during the gradual increase of the coupling strength, the inter-oscillator difference of the system exhibits an obvious fluctuation pattern, and the difference tends to stabilize after a certain coupling strength is reached, showing a plateau period of synchronization. This phenomenon not only demonstrates the effectiveness of the star-shaped coupling mode in facilitating the synchronization of laminar chaotic systems, but also emphasizes the complexity and subtle changes in the internal dynamics of the system during the process of reaching a synchronized state. In particular, it is found that the difference between the peripheral oscillators of the system is significantly smaller than that between the central and peripheral oscillators in the star-coupled mode, a finding that further corroborates the importance of the far-reaching influence of the coupling structure on the synchronization behavior of the system, and at the same time reveals the obvious differences in the dynamical behaviors between the central and peripheral oscillators.

We believe that the results observed in this paper can also be verified experimentally. Further studies are needed in order to explore the complete spectrum of complex synchronization modes in time-varying time-lag systems under diverse coupling conditions, and in the course

of the experiments, more interesting phenomena may be able to be generated.

REFERENCES

1. S. Bagheri and D. S. Henningson. Transition delay using control theory [J]. Philosophical Transactions of the Royal Society A: Mathematical, Physical and Engineering Sciences, 2011; 369(1940): 1365-81.
2. X.-C. Shangguan et al.. Resilient load frequency control of power systems to compensate random time delays and time-delay attacks [J]. IEEE Transactions on Industrial Electronics, 2022; 70(5): 5115-28.
3. S. Luo and Y. Song. analysis-based adaptive backstepping control of the microelectromechanical resonators with constrained output and uncertain time delay [J]. IEEE Transactions on Industrial Electronics, 2016; 63(10): 6217-25.
4. H. Wernecke, B. Sándor, and C. Gros. Chaos in time delay systems, an educational review [J]. Physics Reports, 2019; 824: 1-40.
5. C. P. Chen, G.-X. Wen, Y.-J. Liu, and F.-Y. Wang. Adaptive consensus control for a class of nonlinear multiagent time-delay systems using neural networks [J]. IEEE Transactions on Neural Networks and Learning Systems, 2014; 25(6): 1217-26.
6. L. Jiang, W. Yao, Q. Wu, J. Wen, and S. Cheng. Delay-dependent stability for load frequency control with constant and time-varying delays [J]. IEEE Transactions on Power systems, 2011; 27(2): 932-41.
7. J. Bugler et al. An ignition delay time and chemical kinetic modeling study of the pentane isomers [J]. Combustion and Flame, 2016; 163: 138-56.
8. M. Dehghan and R. Salehi. Solution of a nonlinear time-delay model in biology via semi-analytical approaches [J]. Computer Physics Communications, 2010; 181(7): 1255-65.
9. H. L. Smith. An introduction to delay differential equations with applications to the life sciences [M]. springer New York, 2011.
10. J. W. Peters, A.-F. Miller, A. K. Jones, P. W. King, and M. W. Adams. Electron bifurcation [J]. Current opinion in chemical biology, 2016; 31: 146-52.
11. J. L. Kaplan and J. A. Yorke. Chaotic behavior of multidimensional difference equations [M]. Functional Differential Equations and Approximation of Fixed Points: Proceedings, Bonn, July 1978. Springer. 2006; 204-27.
12. U. Feudel and C. Grebogi. Multistability and the control of complexity [J]. Chaos: An Interdisciplinary Journal of Nonlinear Science, 1997; 7(4): 597-604.
13. D. Müller, A. Otto, and G. Radons. From dynamical systems with time-varying delay to

circle maps and Koopman operators [J]. Physical Review E, 2017; 95(6): 062214.

14. D. Müller, A. Otto, and G. Radons. Laminar chaos [J]. Physical Review Letters, 2018; 120(8): 084102.
15. J. D. Hart, R. Roy, D. Müller-Bender. Laminar chaos in experiments: Nonlinear systems with time-varying delays and noise [J]. Physical Review Letters, 2019; 123(15): 154101.
16. T. Jüngling, T. Stemler, and M. Small. Laminar chaos in nonlinear electronic circuits with delay clock modulation [J]. Physical Review E, 2020; 101(1): 012215.
17. D. Kul'minskii, V. Ponomarenko, and M. Prokhorov. Laminar chaos in a delayed-feedback generator [J]. Technical Physics Letters, 2020; 46: 423-6.
18. V. Ponomarenko, D. Kulminskiy, and M. Prokhorov. Laminar chaos in systems with variable delay time; proceedings of the 2021 5th Scientific School Dynamics of Complex Networks and their Applications (DCNA), F, 2021. [C]. IEEE.
19. T. Khatun, D. Biswas, and T. Banerjee. Synchronization of laminar chaos [J]. The European Physical Journal Plus, 2022; 137(5): 561.
20. C.-U. Choe, T. Dahms, P. Hövel, and E. Schöll. Controlling synchrony by delay coupling in networks: From in-phase to splay and cluster states [J]. Physical Review E, 2010; 81(2): 025205.
21. M. R. Mauricio et al. Synthesis of star poly (N-isopropylacrylamide) by β-cyclodextrin core initiator via ATRP approach in water [J]. Reactive and Functional Polymers, 2011; 71(12): 1160-5.